Low-Force Kinesthetic Guidance for Accurate Positioning and Tracking

Ryo Kikuuwe* Takahiro Yamamoto Hideo Fujimoto

Nagoya Institute of Technology, Nagoya, Aichi 466-8555, Japan

Abstract

This paper considers the application of a low-force robotic manipulator to guide a human user's movement to locate a tool at a predetermined position or to move a tool along a predetermined trajectory. In this application, the guidance must be sufficiently smooth because the user's force can easily overcome the guiding force. The proxy-based sliding mode control, which we previously proposed, is capable of achieving a smooth overdamped convergence to a given position, without overshoots, with a limited actuator torque. This paper proposes the application of the proxy-based sliding mode control to low-force kinesthetic guidance. Experimental results demonstrate the effectiveness of this application, showing that the time constant of the guidance control should be set around 0.1 sec rather than 0.01 sec or 0.5 sec.

CR Categories: H.1.2 [Models and Principles]: User/Machine Systems—Human factors; H.5.2 [Information Interfaces and Presentation]: User Interfaces—Haptic I/O

Keywords: haptic guidance, positioning, sliding mode control, tracking

1 Introduction

Humans and robots have different capabilities. One of the major ideas of human-robot cooperation is to use a robot as a power extender [6, 17] or an intelligent powerful assistant [16]. In this application, a robot produces power following the intention of a human user. That is, a human is in charge of making decisions, while a robot is in charge of producing power. Opposite to this is the approach to use a robot as a passive device that guides a manipulation process performed by a human user [4]. In this approach, a human is in charge of producing power, while a robot is in charge of ensuring the accuracy of the manipulation.

In this paper, we take a different approach in which a human is in charge of producing power, while a robot is in charge of ensuring the accuracy of the manipulation by actively producing small forces. Specifically, we consider the following situation:

1. A human user is required to locate a tool at a given position or to move a tool along a given trajectory.
2. A robot is used to guide the human user's hand toward the target position or along the target trajectory, as illustrated in Fig. 1.
3. The human user knows and can visually recognize the target position or trajectory.
4. The data of the target position or trajectory are provided to the robot controller in advance.
5. The robot's actuators are not strong enough to perform the positioning or tracking task without external forces.

We refer to this application of a robot as *low-force kinesthetic guidance*. Application of robotic devices for guiding human motion have been investigated by several researchers for the purposes of skill training [2, 3, 9, 13, 18] and rehabilitation of upper limb function[10, 11]. In such cases, a low-powered/low-force robot is desirable because a high-powered/high-force robot has potential risks to the user's safety. An active robotic device will be preferred to a passive device if the target position or trajectory is changed according to time.

The low-force kinesthetic guidance scheme has some potential applications even in the manufacturing industry. Because the target position or trajectory is predetermined, full automation without human involvement is technically possible. This scheme, however, can be a solution to remove the spatial isolation of high-powered robots from human workspace. This scheme can be applied to the processes of, for example, cutting, welding, and adhesive/sealant application at specified spots or along a specified trajectory. The isolation of human workers from high-powered robots, which is obliged for the workers' safety, requires a large site area. Moreover, it is inconvenient if the task to be executed by the robot has some subordinate tasks that require human involvement, such as visual/haptic inspection, tool-changing, and fine adjustment. Some researchers have investigated tremor cancellation techniques for assisting accuracy of human manual manipulation [14]. This approach includes technical challenges of separating voluntary movement from involuntary low-frequency errors. The low-force kinesthetic guidance approach can be considered as a solution that is much simpler but limited to the case where the target position or trajectory is given to the device controller in advance.

One might suppose that the low-force kinesthetic guidance involves no technical challenge because it can be accomplished with ordinary stiff position control schemes, such as PD control. However, the choice of the robot control scheme for low-force kinesthetic guidance needs some consideration because the robot's force is assumed to be limited. Under this assumption, the guidance must be performed sufficiently smooth because non-smooth changes in guiding force will cause overshoots in the user's motion even if the robot

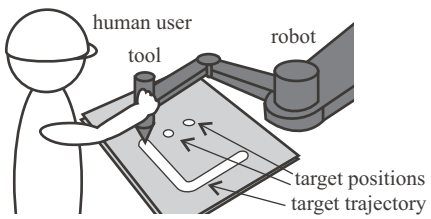

Figure 1: Kinesthetic guidance.

*e-mail: kikuuwe@ieee.org

Symposium on Haptic Interfaces for
Virtual Environment and Teleoperator Systems 2006
March 25 - 26, Alexandria, Virginia, USA
1-4244-0226-3/06/$20.00 ©2006 IEEE

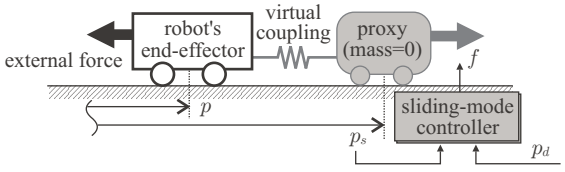

Figure 2: Physical interpretation of proxy-based sliding mode control [8].

tries to stop or change the user's motion. To avoid overshoots, the robot must guide the user to smoothly converge to a target position. A high damping can be a solution to make a smooth movement, but it usually requires a large velocity-feedback gain, which cannot practically be used because the velocity signal is usually noisy especially in low velocity. Moreover, it will deteriorate the tracking capability even below the force limit.

In this paper, we show that the *proxy-based sliding mode control*, which we previously proposed [7, 8], is useful for this application. This control scheme is a modified version of sliding mode control adapted to discrete-time control systems. In this control scheme, the smoothness of coarse (global) guiding action and the responsiveness of fine (local) guiding action can be determined independently from each other. Thus, globally smooth convergent dynamics can be realized without using high velocity feedback gain while maintaining local stiffness and responsiveness. We provide experimental results showing that the time constant of a robotic guidance action should be set around 0.1 sec, which is consistent with previous reports on the frequency range of human voluntary movement. The time constant of 0.1 sec is difficult to be achieved by using ordinary PD control with a very high proportional gain. To our knowledge, the present paper is the first that investigated the influence of the smoothness of the robotic guiding action.

The rest of this paper is organized as follows. Section 2 revisits the theory of the proxy-based sliding mode control. Sections 3 and 4 present experimental results of positioning and trajectory-tracking tasks, respectively. Section 5 provides concluding remarks.

2 Proxy-Based Sliding Mode Control

The proxy-based sliding mode control is a control scheme that has been presented by the authors [7, 8]. This section provides an overview of this control scheme.

2.1 Basic Theory

For simplicity, we start our discussion from a one-dimensional case. Let p_d and p denote the target and actual positions of the robot's end-effector, respectively. Our purpose here is to realize the dynamics that satisfies the following differential equation:

$$p_d - p + H(\dot{p}_d - \dot{p}) = 0, \tag{1}$$

where H is a positive real number. Based on (1), the actual position p asymptotically approaches the target position p_d. The value H acts as the time constant of this asymptotic convergence process. As long as the system develops according to (1), no overshoots occur because (1) is a first order differential equation.

One imaginable way to constraint the object dynamics to (1) is to use a feedback loop with an infinitely high gain, i.e.,

$$f = \lim_{\kappa\to\infty} \left(\kappa(p_d - p) + \kappa H(\dot{p}_d - \dot{p})\right), \tag{2}$$

where f is the actuator force applied to the end-effector. However, because the actuator force f is limited, we must use, instead of (2),

$$f = \lim_{\kappa\to\infty} \min(F, \max(-F, \kappa(p_d - p) + \kappa H(\dot{p}_d - \dot{p}))), \tag{3}$$

where F is a positive real number indicating the limitation of the actuator force. We must notice that (3) is equivalent to

$$f = F\mathrm{sgn}\left((p_d - p) + H(\dot{p}_d - \dot{p})\right). \tag{4}$$

This is one of the simplest examples of the sliding mode control.

The control law of (4) cannot directly be implemented in discrete-time digital control systems because the discontinuity in the sgn element causes chattering. To avoid this, we use an intermediate virtual object, which is termed as a *proxy*, between the real controlled object (the robot's end-effector) and the sliding mode controller, as illustrated in Fig. 2. We assume that the proxy is massless, and its position is denoted by p_s. The robot's end-effector and proxy are connected with a stiff virtual viscoelastic element, which is usually called a virtual coupling [1]. Because the proxy is massless, the force applied from the controller to the proxy is equal to the force applied from the proxy to the end-effector. This means that we have the following algebraic constraints:

$$f = F\mathrm{sgn}\left((p_d - p_s) + H(\dot{p}_d - \dot{p}_s)\right) \tag{5a}$$
$$f = K(p_s - p) + B(\dot{p}_s - \dot{p}), \tag{5b}$$

where K and B are the stiffness and the viscosity of the virtual coupling, respectively.

We derive a discrete-time representation of (5). Let e be defined as

$$e = p_s - p. \tag{6}$$

Then, based on the Euler approximation, we have a discrete-time representation of (5) and (6) as follows:

$$f(k) = F\mathrm{sgn}\left((p_d(k) - p_s(k)) + H(\nabla p_d(k) - \nabla p_s(k))/T\right) \tag{7a}$$
$$f(k) = K(p_s(k) - p(k)) + B(\nabla p_s(k) - \nabla p(k))/T \tag{7b}$$
$$e(k) = p_s(k) - p(k). \tag{7c}$$

Here, k denotes the discrete time index. The operator ∇ is the backward difference operator, which is defined by $\nabla x(k) = x(k) - x(k-1)$. In order to determine $f(k)$ and $e(k)$ with given $p_d(k)$ and $p(k)$, we have to solve the algebraic equations (7). After some derivations, we have the following procedure for solving (7):

$$s(k) = (p_d(k) - p(k)) + H(\nabla p_d(k) - \nabla p(k))/T \tag{8a}$$
$$f_0(k) = \frac{(B + KT)s(k) + (KH - B)e(k-1)}{H + T} \tag{8b}$$
$$f(k) = \begin{cases} f_0(k) & \text{if } |f_0(k)| \le F \\ F\mathrm{sgn}(f_0(k)) & \text{if } |f_0(k)| > F \end{cases} \tag{8c}$$
$$e(k) = \frac{Be(k-1) + Tf(k)}{B + KT}. \tag{8d}$$

If $H = B/K$, this control law reduces to the PD-control scheme with force limit; substituting (8) by $H = B/K$ yields

$$f_0(k) = K(p_d(k) - p(k)) + B(\nabla p_d(k) - \nabla p(k))/T \quad (9a)$$

$$f(k) = \begin{cases} f_0(k) & \text{if } |f_0(k)| \le F \\ F\text{sgn}(f_0(k)) & \text{if } |f_0(k)| > F. \end{cases} \quad (9b)$$

The control law (8) is advantageous over PD control, such as (9), in that the local responsiveness and global smoothness can be set independently. The local responsiveness, which is a characteristic of the recovering motion from a small positional error, is determined by K and B. The global smoothness, which is a characteristic of the recovering motion from a large positional error, is determined by H. We should set $H \gg B/K$. A large value of B/K will deteriorate tracking performance, and a large value of B will increase the undesirable influence of velocity measurement noise. A small H value will cause a fast recovering action from a large positional error, causing overshoots.

2.2 Application to Robotic Systems

The discussion above can easily be extended into multidimensional cases. A vectorial version of (8) can be written as follows:

$$\boldsymbol{s}(k) = (\boldsymbol{p}_d(k) - \boldsymbol{p}(k)) + H(\nabla \boldsymbol{p}_d(k) - \nabla \boldsymbol{p}(k))/T \quad (10a)$$

$$\boldsymbol{f}_0(k) = \frac{(B + KT)\boldsymbol{s}(k) + (KH - B)\boldsymbol{e}(k-1)}{H + T} \quad (10b)$$

$$\boldsymbol{f}(k) = \begin{cases} \boldsymbol{f}_0(k) & \text{if } \|\boldsymbol{f}_0(k)\| \le F \\ F\boldsymbol{f}_0(k)/\|\boldsymbol{f}_0(k)\| & \text{if } \|\boldsymbol{f}_0(k)\| > F \end{cases} \quad (10c)$$

$$\boldsymbol{e}(k) = \frac{B\boldsymbol{e}(k-1) + T\boldsymbol{f}(k)}{B + KT}, \quad (10d)$$

where bold-face symbols denote vectors correspondent to scalars in (8). In this case, the force limit is specified in terms of the magnitude of the force vector. That is, $\boldsymbol{f}(k)$ is determined to satisfy $\|\boldsymbol{f}(k)\| < F$.

In a multi-linkage mechanism, (10) should be slightly modified because the force limit should usually be specified in terms of the torque of each actuator. In (10), assume that $\boldsymbol{p}$ and $\boldsymbol{p}_d$ are the actual and target positions of the end-effector in the Cartesian coordinate system, and $\boldsymbol{f}$ is the force vector produced at the end-effector. Let $\boldsymbol{J}$ be the Jacobean matrix that transforms the joint angular velocity to the end-effector velocity in Cartesian space. Then, the joint actuator torque that is statically equivalent to $\boldsymbol{f}$ is described as $\boldsymbol{\tau} = \boldsymbol{J}^T\boldsymbol{f}$. By using this, we have the modified version of (10) in which the force limit is specified in terms of the actuator torque, which is written as follows:

$$\boldsymbol{s}(k) = (\boldsymbol{p}_d(k) - \boldsymbol{p}(k)) + H(\nabla \boldsymbol{p}_d(k) - \nabla \boldsymbol{p}(k))/T \quad (11a)$$

$$\boldsymbol{f}_0(k) = \frac{(B + KT)\boldsymbol{s}(k) + (KH - B)\boldsymbol{e}(k-1)}{H + T} \quad (11b)$$

$$\boldsymbol{\tau}_0(k) = \boldsymbol{J}^T\boldsymbol{f}_0(k) \quad (11c)$$

$$\boldsymbol{\tau}(k) = \begin{cases} \boldsymbol{\tau}_0(k) & \text{if } \|\boldsymbol{\tau}_0(k)\|_\infty \le F_\tau \\ F_\tau\boldsymbol{\tau}_0(k)/\|\boldsymbol{\tau}_0(k)\|_\infty & \text{if } \|\boldsymbol{\tau}_0(k)\|_\infty > F_\tau \end{cases} \quad (11d)$$

$$\boldsymbol{f}(k) = \boldsymbol{J}^{-T}\boldsymbol{\tau}(k) \quad (11e)$$

$$\boldsymbol{e}(k) = \frac{B\boldsymbol{e}(k-1) + T\boldsymbol{f}(k)}{B + KT}. \quad (11f)$$

Here, F_τ is the positive real number that indicates the limit of the actuator torque, and $\|\boldsymbol{x}\|_\infty$ denotes the L-infinity norm of $\boldsymbol{x}$, which returns $\max_i |x_i|$, where x_i is the i-th element of $\boldsymbol{x}$.

If $H = B/K$, (11) becomes equivalent to

$$\boldsymbol{f}_0(k) = K(\boldsymbol{p}_d(k) - \boldsymbol{p}(k)) + B(\nabla \boldsymbol{p}_d(k) - \nabla \boldsymbol{p}(k))/T \quad (12a)$$

$$\boldsymbol{\tau}_0(k) = \boldsymbol{J}^T\boldsymbol{f}_0(k) \quad (12b)$$

$$\boldsymbol{\tau}(k) = \begin{cases} \boldsymbol{\tau}_0(k) & \text{if } \|\boldsymbol{\tau}_0(k)\|_\infty \le F_\tau \\ F_\tau\boldsymbol{\tau}_0(k)/\|\boldsymbol{\tau}_0(k)\|_\infty & \text{if } \|\boldsymbol{\tau}_0(k)\|_\infty > F_\tau \end{cases} \quad (12c)$$

$$\boldsymbol{f}(k) = \boldsymbol{J}^{-T}\boldsymbol{\tau}(k). \quad (12d)$$

This is a PD position control law in Cartesian coordinate system with bounded joint torques.

2.3 Application to Kinesthetic Guidance

When the control law (11) is used for kinesthetic guidance, the parameters in (11) should be carefully chosen. The force limit F_τ is usually determined by the hardware limitations or for safety reasons. The proportional feedback gain K should be chosen as high as possible. The derivative feedback gain B should be chosen as small as possible but large enough to suppress oscillation.

The most important is the parameter H. It is the time constant of the convergent dynamics to be realized, which is described as (1). The H value determines the smoothness of the guidance. Therefore, it should be chosen based on how smooth the human voluntary movement is.

The literature includes several reports on the frequency range of human voluntary movement. Mann et al. [12] measured the wrist motion for 24 activities of daily living using electrogoniometer attached to the wrist. They concluded that the predominant frequency component of the wrist motion for these activities was 1 Hz, and 75% of the spectral energy was less than 5 Hz. Hollerbach [5] measured hand movements during writing letters using an X-Y sliding rail system equipped with accelerometers. In their data, the frequency of the motions is no higher than 7 Hz. Riviere et al. [15] measured hand motions of trained eye surgeons performing a simulated microsurgery on a mannequin eye. They concluded that 98.9% of the total power of voluntary movements was below 2 Hz.

Roughly speaking, by viewing a human as a first-order delay system with cut-off frequency of 2 Hz, we can assume that the time constant of the convergent process in reaching motions would be $1/(2\pi \times 2) = 0.08$ sec. Therefore, we can assume that an optimal value for H should be, very roughly, around 0.1 sec.

3 Experiment I: Positioning Task

We performed preliminary experiments to test the effectiveness of the proxy-based sliding mode control in low-force kinesthetic guidance. This section describes experiments to test its application to a positioning task, and the next section descries that to a tracking task.

The purpose of these experiments is to show the advantage of the proxy-based sliding mode control, which is described by (11), over the PD position control with force limit, which is described by (12). Notice that (12) is a special case of (11) with $H = B/K$. Therefore, we attempt to show that the H value in (11) should be chosen as $H \gg B/K$ for kinesthetic guidance.

3.1 Setup

We used the 2-DOF planar parallel manipulator shown in Fig. 3. This manipulator had two actuators on the joints,

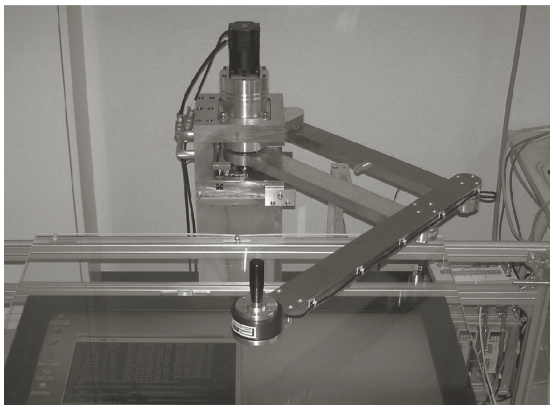

(a) manipulator and LCD monitor.

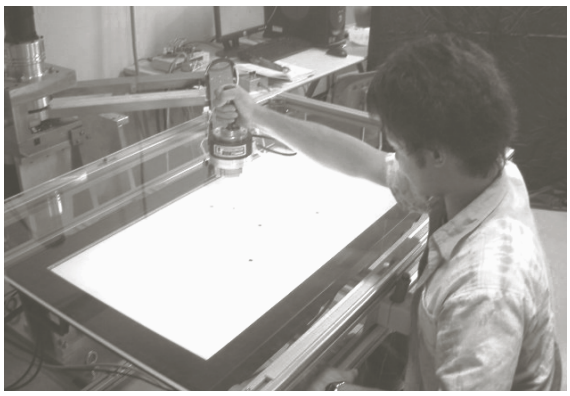

(b) a participant using the manipulator.

Figure 3: Photographs of experimental setup.

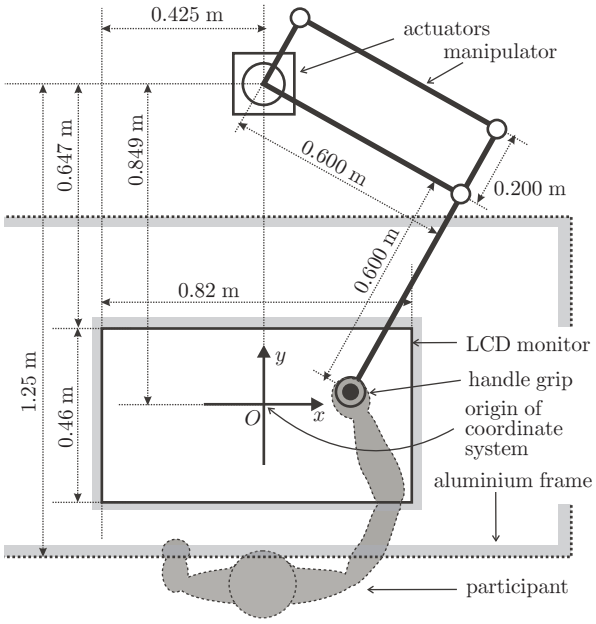

(a) top view.

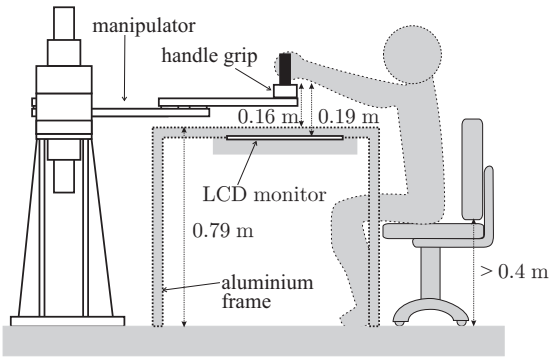

(b) side view.

Figure 4: Dimensions of experimental setup.

which were AC servomotors with Harmonic drive gearings. This manipulator had large friction in its joints (approximately 10 Nm). A handle grip was attached to the end-effector. An LCD monitor was placed horizontally about 0.2 m below the handle grip. The manipulator and the LCD monitor were arranged as shown in Fig. 4. The whole system was controlled using a personal computer running ART-Linux. The position of the end-effector was measured with two optical encoders attached to the joint actuators. No force/torque sensors were used for control or measurement.

3.2 Methods and Stimuli

Eight male volunteers participated in the experiment I. All participants were university or graduate students. All of them classified themselves as right handed, and had no known injury in their right arms.

As shown in Fig. 5, the LCD monitor displayed 4 solid circles with diameters 0.009 m. One of the circles, PC, was located at $[0\,\mathrm{m}, -0.05\,\mathrm{m}]^T$. The other three circles, P0, P1, and P2, were at the vertices of an equilateral triangle with $0.15 \times \sqrt{3}$ m sides centered at PC. A blue solid circle with diameter 0.008 m was drawn immediately below the end-effector to indicate the position of the end-effector. The participants were asked to move the end-effector from PC to a target position as quickly as possible. The target position was randomly chosen out of P0, P1, and P2. The solid circles of P0, P1, and P2 were drawn in red when chosen as the target position, in black otherwise.

The manipulator was controlled using the control law described by (11); the end-effector's position in the Cartesian coordinate system measured by the optical encoders was used as the input position $\boldsymbol{p}$, and the output torque $\boldsymbol{\tau}$ was commanded to the actuators. Six parameter settings, C0 to C5, listed in Table 1, were used. The sampling interval was $T = 0.001$ sec. Notice that the manipulator was not actuated with the setting C0, and that the torque limit $F_\tau = 7$ N (in the settings C1 to C5) was lower than the joint friction level; the manipulator hardly moved without external forces. As we explained in section 2.3, $H = 0.1$ sec is expected to be a suitable value for kinesthetic guidance. In addition, we can infer that a high K value will contribute accurate positioning. Thus, the setting C2 is expected to be the best among the 6 settings in Table 1. The proportional gain of $K = 60000$ N/m was close to the highest value for which the entire system was stable.

A single trial of the experiment was performed in the following procedure:

step 1 The end-effector was fixed at PC.

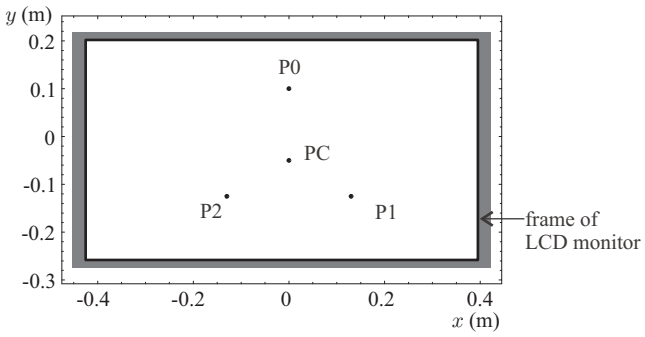

Figure 5: Graphic representation during experiment I.

Table 1: Parameter settings used in the experiments.

name	F_τ (Nm)	H (s)	K (N/m)	B (Ns/m)
C0	0	–	–	–
C1	7	0.5	60000	210
C2	7	0.1	60000	210
C3	7	0.01	60000	210
C4	7	0.1	6000	210
C5	7	0.1	600	210

step 2 A three-second countdown was given with beep sounds.

step 3 At the instant of the "start" beep ($t = 0$), one of P0 to P2 was chosen as the target position and was turned red. The control law (11) was activated with one of the settings C0 to C5. The participant moved the end-effector to the target position.

step 4 After the end-effector's staying within 0.0005 m of the target position (i.e., the blue circle's staying within the red circle) for 0.5 sec ($t = \mathcal{A}$), the end-effector was judged to reach the target.

step 5 The end-effector was moved to PC. After a 3-second interval, step 2 was repeated.

For each trial, the time length $\mathcal{A}$ and the traveled path length $\mathcal{D} = \int_0^{\mathcal{A}} \|\dot{\boldsymbol{p}}(t)\| dt$ were recorded.

Every single participant performed 18 trials. All of 18 possible combinations of the 6 settings (C0 to C5) and 3 target positions (P0, P1, and P2) were presented to each participant. The order of presentation was randomized for each participant.

Table 2: Results of experiment I: Two-sided p-values based on Welch's t-tests.

comparison	difference in $\mathcal{A}$ (p-values)	difference in $\mathcal{D}$ (p-values)
C3-C2	2.51×10^{-1}(ns)	2.59×10^{-5}(**)
C2-C1	5.70×10^{-16}(**)	9.27×10^{-2}(ns)
C1-C0	3.10×10^{-5}(**)	2.35×10^{-3}(**)
C0-C5	7.61×10^{-3}(**)	2.32×10^{-7}(**)
C5-C4	1.01×10^{-1}(ns)	8.40×10^{-3}(**)
C4-C2	2.94×10^{-2}(*)	3.60×10^{-1}(ns)

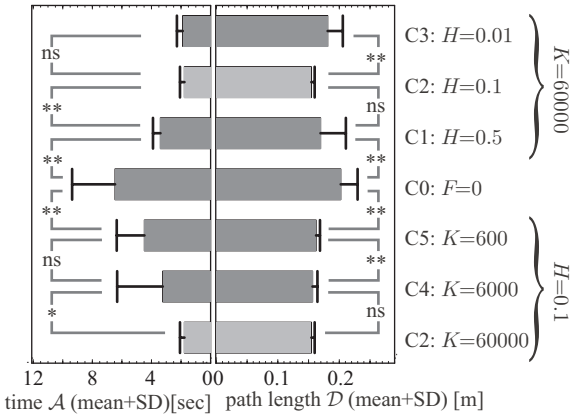

Figure 6: Results of experiment I.

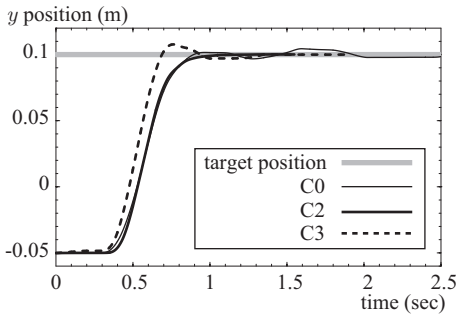

Figure 7: Sample data of experiment I.

3.3 Results

The total number of trials under each setting of C0 to C5 was 24 (3 trials × 8 participants). The averages and the standard deviations of the time $\mathcal{A}$ and the path length $\mathcal{D}$ under the settings C0 to C5 are shown in Fig. 6. Note that they are in an order convenient for comparison, and that the result with the setting C2 is presented at two places. The results were analyzed using Welch's t-test because the variance cannot be assumed to be equal among settings. The p-values for the comparisons are shown in Table 2. In both of Fig. 6 and Table 2, the single asterisk (*) and double asterisk (**) indicate significant differences at $p < 0.05$ and $p < 0.01$, respectively, and ns indicates no significant difference ($p \geq 0.05$).

The performance under the setting C0 is significantly worse than those under the other settings. This means that even a small guiding force below the static friction level can improve the efficiency of positioning tasks.

Among the settings C1, C2, and C3, which have a common K value, the setting C2 ($H = 0.1$ sec) created the best result. This result supports our discussion in section 2.3. The difference between C2 and C3 is not significant in time length $\mathcal{A}$, but is significant in the path length $\mathcal{D}$. This indicates that a small H value ($H = 0.01$ sec in C3) can increase the speed of the reaching motion but can cause overshoots. Fig. 7 shows a participant's motions from PC to P1 under the settings C0, C2, and C3. It is apparent that the position approaches to the target position P1 faster under the

setting C3 than under the setting C2, but the setting C3 results in overshoots. The setting C2 creates more smooth and efficient movement than the settings C0 and C3.

The comparison among C2, C4, and C5 suggests that a large K value is desirable for guiding positioning tasks. This is likely because, as the K value increases, the force attracting the end-effector to the target position becomes larger up to the saturation level determined by F_τ.

4 Experiment II: Tracking Task

We performed another experiment to test the effectiveness of the proxy-based sliding mode control for low-force kinesthetic guidance of trajectory-tracking tasks. We also used the setup which is introduced in section 3.1 and shown in Fig. 3 and Fig. 4. The control law (11) was used also in this experiment with the parameter settings C0 to C5 in Table 1.

4.1 Methods and Stimuli

Eight male volunteers participated in this experiment. All participants were university or graduate students. All of them classified themselves as right handed, and had no known injury in their right arms.

The target trajectory to be tracked was chosen as shown in Fig. 8, which is a Lissajou's curve described as follows:

$$\boldsymbol{p}_d(t) = [A_x \sin(\Omega t),\ A_y \sin(2\Omega t) + B_y]^T, \qquad (13)$$

where $A_x = 0.25$ m, $A_y = 0.15$ m, $B_y = -0.06$ m, $\Omega = \pi/2$ rad/sec. A single trial of the experiment includes 2 laps around the trajectory (i.e., $t \in [0\,\text{sec}, 8\,\text{sec}]$). This trajectory was drawn as a red solid curve. The target position $\boldsymbol{p}_d$ at each time instant was indicated by a solid red circle with diameter 0.012 m. In addition, a solid blue circle with diameter 0.008 m was drawn immediately below the end-effector to indicate the measured end-effector position $\boldsymbol{p}$.

A single trial of this experiment was performed in the following procedure:

step 1 The end-effector position was fixed at the position $[0, B_y]^T$.

step 2 A three-second countdown was given with beep sounds.

step 3 At the instant of the "start" beep ($t = 0$), the red circle started to move along the trajectory (13). The control law (11) was activated with one of the settings C0 to C5. The participant started to move the end-effector to follow the red circle as accurately as possible.

step 4 After 2 cycles ($t = 8$ sec), step 1 was repeated.

Every single participant performed 6 trials. All of 6 settings (C0 to C5) were presented to each participant. The order of presentation was randomized for each participant.

4.2 Results

We choose the following criteria for evaluating the result of a single trial:

$$\mathcal{L} = \frac{1}{t_1 - t_0} \int_{t_0}^{t_1} \ln(\|\boldsymbol{p}(t) - \boldsymbol{p}_d(t)\|) dt, \qquad (14)$$

where $t_0 = 0.4$ sec, $t_1 = 7.6$ sec, and $\|\boldsymbol{p}(t) - \boldsymbol{p}_d(t)\|$ is measured in meters (m). The differences in $\mathcal{L}$ among participants were quite large compared to those according to the settings, probably because this task depends on physical capabilities.

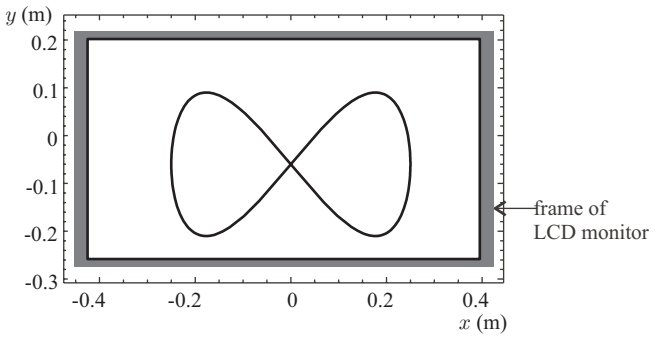

Figure 8: Graphic representation during experiment II.

In order to cancel such influence, we subtracted the average of the $\mathcal{L}$ values within each participant from the $\mathcal{L}$ values of every trial. That is, we used the following criteria to evaluate the i-th trial of the j-th participant:

$$\mathcal{N}_{i,j} = \mathcal{L}_{i,j} - (\mathcal{L}_{0,j} + \cdots + \mathcal{L}_{5,j})/6, \qquad (15)$$

where $\mathcal{L}_{i,j}$ denotes the $\mathcal{L}$ value of the i-th trial ($i = 0, \cdots, 5$) of the j-th participant.

The total number of trials under each setting of C0 to C5 was 8 (1 trial $\times$ 8 participants). Fig 9 shows the averages and the standard deviations of the $\mathcal{N}$ values under the settings C0 to C5. They are in the same order as in Fig. 6. Welch's t-test comparisons are shown in Table 3. In both of Fig. 9 and Table 3, the single asterisk (*) and double asterisk (**) indicate significant differences at $p < 0.05$ and $p < 0.01$, respectively, and ns indicates no significant difference ($p \geq 0.05$).

The setting C2 created the result better than the other settings. This results show that, in order to reduce the tracking error, the proportional gain K should be chosen as high as possible, and H should be around 0.1 sec. This result is consistent with out discussion in section 2.3. Fig. 10 shows a participant's motions under the settings C0, C2, and C3. It is apparent that the setting C2 creates the best results, and the setting C3, which includes a small H values, results in a oscillatory motion due to repeated overshoots.

As a supplementary experiment, we tried the parameter setting $F = 7$ Nm, $K = 60000$ N/m, $B = 6000$ Ns/m, and $H = 0.1$ sec. This parameter setting is the same in K and H as the setting C2, but because of $H = B/K$, this makes the control law (11) to be equivalent to (12), which is PD control with bounded actuator torques. With this parameter setting, the actuator often created undesirable noisy sound especially when the position force was very close to the target position and the target velocity was very low. It is probably because the large B value amplified the influence of the measurement noise in the velocity signal. This indicates that the proxy-based sliding mode control is a necessary choice to realize a high damping and a high stiffness with an appropriate damping-stiffness ratio (i.e., time constant).

5 Conclusion

This paper has proposed the application of the proxy-based sliding mode control, which we previously proposed [8], to low-force kinesthetic guidance for accurate positioning and tracking. The advantage of the proxy-based sliding mode control over the ordinary PD control scheme is that it can

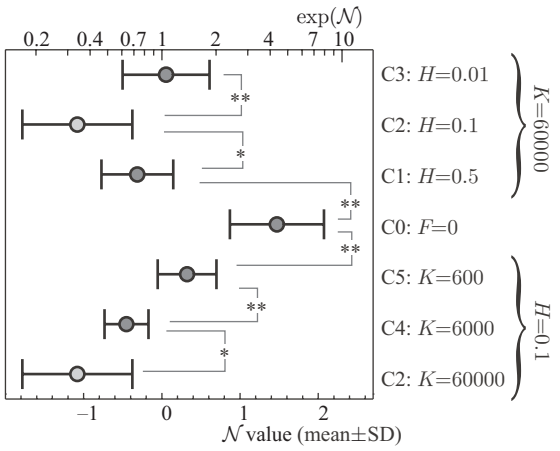

Figure 9: Results of experiment II.

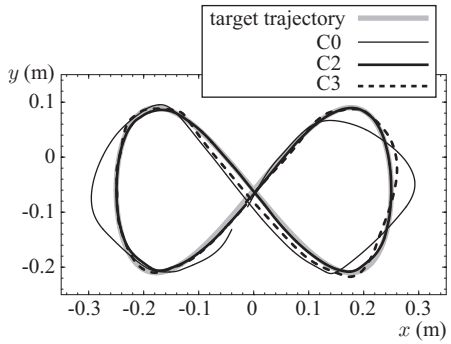

Figure 10: Sample data of experiment II.

realize a globally smooth convergent dynamics without using high velocity feedback gain while maintaining local stiffness and responsiveness. Two experiments were performed to test this application. The results showed that the parameter H, which represents the time constant of the global convergent dynamics achieved by this guidance, should be set around 0.1 sec rather than 0.01 sec or 0.5 sec, indicating a degree of smoothness suitable for a robotic guiding action. It was also shown that the parameter K, which determines the local stiffness of the guidance, should be set as high as possible. The parameter B, which represents the local damping coefficient, was set low not to deteriorate local responsiveness or not to be affected by the noise in velocity signals.

We have discussed the choice of the time constant H in relation to the frequency characteristics of human movement.

Table 3: Results of experiment II: Two-sided P-values based on Welch's t-tests.

comparison	p-values
C3-C2	3.26×10^{-3}(**)
C2-C1	2.40×10^{-2}(*)
C1-C0	1.48×10^{-5}(**)
C0-C5	6.67×10^{-4}(**)
C5-C4	4.42×10^{-4}(**)
C4-C2	4.32×10^{-2}(*)

However, it will be certain that such characteristics depend on the state of muscle contraction. Human's sensitivity to the H value used in guidance should be investigated. If the performance of task execution is sufficiently insensitive to the H value, we can use a fixed H value irrespective of the state of muscle contraction.

The low-force kinesthetic guidance scheme using the proxy-based sliding mode control can also be effective for motor skill teaching to human users and for sensorimotor training in rehabilitation. In such applications, there is expected to be a need to weaken the guidance force as the learning or training process progresses. The smoothness of guidance action will be especially required when the force is set small, and this will increase the necessity for the proxy-based sliding mode control. Effectiveness of such applications and the choice of parameter values for the control law should be investigated in future study.

References

[1] J. E. Colgate, M. C. Stanley, and J. M. Brown. Issues in the haptic display of tool use. In *Proc. of 1995 IEEE/RSJ Int. Conf. on Intelligent Robots and Systems*, pages 140–145, 1995.

[2] D. Feygin, M. Keehner, and F. Tendick. Haptic guidance: Experimental evaluation of a haptic training method for a perceptual motor skill. In *Proc. of 10th Symp. on Haptic Interfaces for Virtual Environment and Teleoperator Systems*, pages 40–47, 2002.

[3] B. Forsyth and K. E. MacLean. Predictive haptic guidance: Intelligent user assistance for the control of dynamic tasks. *IEEE Trans. on Visualization and Computer Graphics*, 12(1):103–113, 2006.

[4] R. B. Gillespie, J. E. Colgate, and M. A. Peshkin. A general framework for cobot control. *IEEE Trans. on Robotics and Automation*, 17(4):391–401, 2001.

[5] J. M. Hollerbach. An oscillation theory of handwriting. *Biological Cybernetics*, 39:139–156, 1981.

[6] H. Kazerooni. Human-robot interaction via the transfer of power and information signals. *IEEE Trans. on Systems, Man and Cybernetics*, 20(2):450–463, 1990.

[7] R. Kikuuwe and H. Fujimoto. Discrete-time sliding mode control with finite-time sliding-mode reaching. In *Proc. of the 23rd Annual Conf. of the Robotics Society of Japan*, 3A16, 2005 (in Japanese).

[8] R. Kikuuwe and H. Fujimoto. Proxy-based sliding mode control for accurate and safe position control. In *Proc. of 2006 IEEE Int. Conf. on Robotics and Automation*, 2006 (accepted).

[9] R. Kikuuwe and T. Yoshikawa. Haptic display device with fingertip presser for motion/force teaching to human. In *Proc. of 2001 IEEE Int. Conf. on Robotics and Automation*, pages 868–873, 2001.

[10] H. I. Krebs, N. Hogan, M. L. Aisen, and B. T. Volpe. Robot-aided neurorehabilitation. *IEEE Trans. on Rehabilitation*, 6(1):75–87, 1998.

[11] J. Liu, J. L. Emken, S. C. Cramer, and D. J. Reinkensmeyer. Learning to perform a novel movement pattern using haptic guidance: Slow learning, rapid forgetting, and attractor paths. In *Proc. of IEEE 9th Int. Conf. on Rehabilitation Robotics*, pages 37–40, 2005.

[12] K. A. Mann, F. W. Wernere, and A. K. Palmer. Frequency spectrum analysis of wrist motion for activities of daily living. *J. of Orthopaedic Research*, 7(2):304–306, 1989.

[13] M. K. O'Malley and K. Gupta. Passive and active assistance for human performance of a simulated underactuated dynamic task. In *Proc. of 11th Symp. on Haptic Interfaces for Virtual Environment and Teleoperator Systems*, pages 348–355, 2003.

[14] C. N. Riviere and P. K. Khosla. Augmenting the human-machine interface: improving manual accuracy. In *Proc. of 1997 IEEE Int. Conf. on Robotics and Automation*, pages 3546–3550, 1997.

[15] C. N. Riviere, R. S. Rader, and P. K. Khosla. Characteristics of hand motion of eye surgeons. In *Proc. of 19th Annual Conf. of the IEEE Engineering in Medicine and Biology Society*, volume 4, pages 1690–1693, 1997.

[16] T. Tsumugiwa, R. Yokogawa, and K. Hara. Variable impedance control based on estimation of human arm stiffness for human-robot cooperative calligraphic task. In *Proc. of 2002 IEEE Int. Conf. on Robotics and Automation*, pages 644–650, 2002.

[17] Y. Yamada, H. Konosu, T. Morizono, and Y. Umetani. Proposal of skill-assist: A system of assisting human workers by reflecting their skills in positioning tasks. In *Proc. of 1999 IEEE Int. Conf. on Systems, Man, and Cybernetics*, volume 4, pages 11–16, 1999.

[18] Y. Yokokohji, R. L. Hollis, T. Kanade, K. Henmi, and T. Yoshikawa. Toward machine mediated training of motor skills -skill transfer from human to human via virtual environment-. In *Proc. of 5th IEEE Int. Workshop on Robot and Human Interactive Communication*, pages 32–37, 1996.